Unified Impedance and Admittance Control

Christian Ott, Ranjan Mukherjee, and Yoshihiko Nakamura

Abstract— Impedance and Admittance Control are two distinct implementations of the same control goal. It is well known that their stability and performance properties are complementary. In this paper, we present a hybrid system approach, which incorporates Impedance and Admittance Control as two extreme cases of one family of controllers. This approach allows to continuously switch and interpolate between Impedance and Admittance Control. We compare the basic stability and performance properties of the resulting controllers by means of an extensive case study of a one-dimensional system and present an experimental evaluation using the KUKA-DLR-lightweight arm.

I. INTRODUCTION

The most successful applications of industrial robots are primarily restricted to tasks where there is virtually no energy exchange between the robot and its environment. Robotic manipulation tasks in which energy is exchanged with the environment through dynamic interaction has been a subject of considerable research and two fundamental control methodologies have been proposed. The first approach, known as "Hybrid Position and Force Control," was developed by Raibert and Craig [1]. The compliance control methodology of Mason [2] is a variation of this approach. In hybrid position and force control, the task space is divided into position-controlled and force-controlled subspaces since both position and force cannot be controlled along any given direction. The hybrid position and force control methodology ignores the dynamic coupling between the manipulator and the environment and as a result it is not possible to control the commanded position or force accurately. To address this problem, Hogan proposed "Impedance Control" [3], wherein the mechanical impedance of the manipulator is regulated to that of a target model. Impedance control establishes a dynamical relationship between the end-effector position and force.

Efforts have been made to combine impedance control and hybrid position and force control. Anderson and Spong [4] proposed an inner/outer loop control strategy; the inner loop is based on feedback linearization with force cancellation and the outer loop is similar to the classical hybrid position and force controller [1] with impedance control in the position-controlled subspace. Liu and Goldenberg [5] proposed a robust hybrid controller with impedance control in the position-controlled subspace and desired inertia and damping in the force-controlled subspace to improve dynamic behavior.

There are two ways of implementing impedance control, depending on the causality of the controller. These are often referred to as "Impedance Control" and "Admittance Control" in the literature. Although both implementations were referred to as impedance control by Hogan [3], we make a distinction since it is central to the work presented here. In Impedance Control the controller is an impedance[1] and the manipulator is an admittance and in Admittance Control the controller is an admittance and the manipulator is an impedance. The stability properties of Impedance and Admittance Control in the presence of non-ideal effects such as time delay was discussed by Lawrence [6].

In general, robotic systems with Impedance Control have stable dynamic interaction with stiff environments but have poor accuracy in free-space due to friction and other unmodeled dynamics. This problem can be mitigated using inner loop torque sensing/control or through hardware modifications such as low-friction joints and direct-drive actuators. Impedance Control has been implemented with inner loop torque sensing and control in DLR's light-weight robot [7] and ATR's[2] Humanoid built by Sarcos[3] [8]; and with low-friction joints and low inertia in the Phantom[4] haptic device. In contrast to Impedance Control, Admittance Control provides high level of accuracy in non-contact tasks but can result in instability during dynamic interaction with stiff environments. This problem can be eliminated using series elastic actuation or compliant end-effectors but this reduces performance. In contrast to direct-drives which are used in conjunction with Impedance Control, Admittance Control requires high transmission ratios such as harmonic drives for precise motion control, and industrial robotic systems are good examples.

Robotic systems with Impedance Control and Admittance Control have complementary advantages and disadvantages. It is possible to improve the performance of both control algorithms through specific hardware modifications but such modifications result in a predisposition to Impedance Control or Admittance Control. To have no predisposition and instead have complete flexibility in choosing the "best" controller for any given task, we propose a control strategy that unifies Impedance Control and Admittance Control based on a hy-

Ch. Ott is with the Institute of Robotics and Mechatronics, German Aerospace Center (DLR), P. O. Box 1116, D-82230 Wessling, Germany, email: christian.ott@dlr.de

R. Mukherjee is with the Department of Mechanical Engineering, Michigan State University, East Lansing, MI, 48824, USA, and is the corresponding author, email: mukherji@egr.msu.edu

Y. Nakamura is with the Department of Mechano-Informatics, University of Tokyo, 7-3-1 Hongo, Bunkyo-ku, Tokyo 113, Japan

[1]A physical system that accepts motion inputs and yields force outputs is defined as an impedance. A system that accepts force inputs and yields motion outputs is defined as an admittance [3].

[2]Advanced Telecommunications Research Institute International - Japan

[3]www.sarcos.com

[4]product of SensAble Technologies, Inc., www.sensable.com

brid systems framework [9]. Our approach results in a continuous spectrum of hybrid controllers with Impedance Control and Admittance Control at two ends of the spectrum. We do not discuss the procedure for choosing the "best" controller for a given task and environment but derive conditions for stability of dynamic interaction and stability of the switched system. Through numerical simulations and experimental results it is shown that our hybrid control designs improve stability and performance characteristics of interaction controllers which has been restricted to Impedance Control and Admittance Control thus far.

II. BACKGROUND

A. Problem Statement

Consider a single degree-of-freedom system in which a mass interacts with an environment. Let m and x be the generalized inertia and displacement of the mass, respectively, and let F and F_{ext} be the control force and external force of the environment acting on the mass. The equation of motion of the mass can be written as follows

$$m\ddot{x} = F + F_{\text{ext}} \tag{1}$$

The control objective for both Impedance and Admittance Control is to design the control force F that will establish a given relationship between the external force F_{ext} and the deviation $e = (x - x_0)$ from a desired equilibrium trajectory x_0. Typically, a linear second-order relationship of the form

$$M_d\ddot{e} + D_d\dot{e} + K_d e = F_{\text{ext}} \tag{2}$$

is considered, where the positive constants M_d, D_d, and K_d represent the desired "inertia"[5], damping, and stiffness, respectively. While the general concept of impedance control allows to use more general impedance behaviors, in many robotics applications the restriction of the desired behavior to the linear form (2) is sufficient.

B. Impedance Control

In Impedance Control, the controller is a mechanical impedance and consequently the controlled plant is treated as an admittance (see Fig. 1). By comparing (1) with the desired behavior (2), we can derive the Impedance Control law as

$$F = \left(\frac{m}{M_d} - 1\right) F_{\text{ext}} + m\ddot{x}_0 - \frac{m}{M_d}(D_d\dot{e} + K_d e) \tag{3}$$
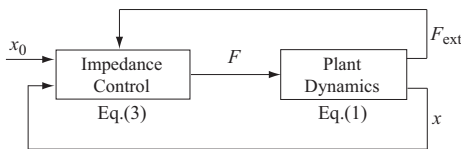

Fig. 1.   Implementation of Impedance Control.

[5]To be precise, $M_d\ddot{e}$ can be interpreted as an *inertial* force only for $\ddot{x}_0 = 0$.

C. Admittance Control

In Admittance Control, the plant is position-controlled and behaves as a mechanical impedance. Hence the controller is designed to be a mechanical admittance (see Fig. 2).
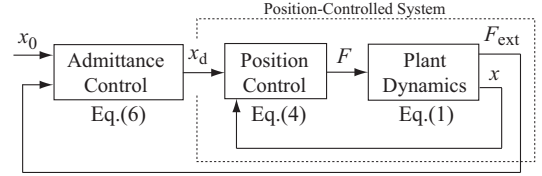

Fig. 2.   Implementation of Admittance Control.

The position controller can be implemented using a PD regulation controller (see [6], for example) of the form

$$F = k_p(x_d - x) - k_d\dot{x} \tag{4}$$

with positive gains k_p and k_d and the desired position x_d. Substituting (4) into (1) and rewriting (2) after replacing x with x_d, the complete system dynamics can be written as follows

$$m\ddot{x} + k_d\dot{x} + k_p(x - x_d) = F_{\text{ext}} \tag{5}$$

$$M_d(\ddot{x}_d - \ddot{x}_0) + D_d(\dot{x}_d - \dot{x}_0) + K_d(x_d - x_0) = F_{\text{ext}} \tag{6}$$

III. HYBRID SYSTEM FRAMEWORK

A. Motivation

Impedance Control provides very good performance when the environment is stiff but results in poor accuracy when the environment is soft. In contrast, Admittance Control provides very good performance for soft environments but results in contact instability for stiff environments. The complementary characteristics of the two controllers is well known (see, e.g., [10]) and is qualitatively illustrated in Fig.3. Both Impedance Control and Admittance Control result in unsatisfactory performance when there are large changes in the stiffness. This limitation can be attributed to their fixed causality. An ideal controller should provide consistently good performance, independent of the environment stiffness. In the next section we propose a control strategy that overcomes the limitations of fixed-causality controllers by continually switching between impedance and admittance causality.
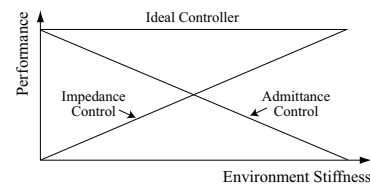

Fig. 3.   Qualitative illustration of the performance of Impedance Control and Admittance Control for different environment stiffness

555

B. Framework

For the single degree-of-freedom system described by (1), we propose to switch the controller between impedance and admittance causality as follows

$$F = \begin{cases} F_1 : t_0 + k\delta \leq t < t_0 + (k+1-n)\delta \\ F_2 : t_0 + (k+1-n)\delta \leq t < t_0 + (k+1)\delta \end{cases} \quad (7)$$

where t_0 is the initial time, δ is the switching period, $n \in [0,1]$ is the duty cycle, k is an integer that takes on values $0, 1, \cdots, F_1$ is the static state feedback law given by (3), and F_2 is the dynamic controller described by (4) and (6). This is explained with the help of Fig.4.
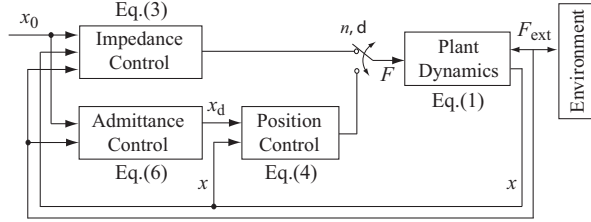

Fig. 4. Controller switching between impedance and admittance causality

With Impedance Control, the closed-loop system behavior is described by (2). With Admittance Control, the closed-loop system behavior is described by (5) and (6). If the environment is modeled as a linear spring

$$F_{\text{ext}} = -k_e(x - x_0) = -k_e e \quad (8)$$

and the virtual equilibrium position is assumed fixed, *i.e.*,

$$\dot{x}_0 = \ddot{x}_0 = 0 \quad (9)$$

the hybrid system has the following descriptions

$$\begin{aligned} \dot{X}_i = A_i X_i &: t_0 + k\delta \leq t < t_0 + (k+1-n)\delta \\ \dot{X}_a = A_a X_a &: t_0 + (k+1-n)\delta \leq t < t_0 + (k+1)\delta \end{aligned} \quad (10)$$

where $X_i = (e \ \dot{e})^T$, $X_a = (e \ \dot{e} \ e_d \ \dot{e}_d)^T$, $e_d = (x_d - x_0)$ and

$$A_i = \begin{bmatrix} 0 & 1 \\ -(K_d + k_e)/M_d & -D_d/M_d \end{bmatrix}$$

$$A_a = \begin{bmatrix} 0 & 1 & 0 & 0 \\ -(k_p + k_e)/m & -k_d/m & k_p/m & 0 \\ 0 & 0 & 0 & 1 \\ -k_e/M_d & 0 & -K_d/M_d & -D_d/M_d \end{bmatrix}$$

When the system switches from Impedance to Admittance Control, two additional states are introduced. These states, e_d and $\dot{e}_d$, are conveniently chosen to maintain continuity in the control force F and its derivative. Equation (4), which gives the expression for the control force in Admittance Control,

can be written as follows

$$\begin{aligned} x_d &= x + \frac{1}{k_p}(F + k_d\dot{x}) \\ \Rightarrow e_d &= e + \frac{1}{k_p}(F + k_d\dot{e}) \\ \dot{x}_d &= \dot{x} + \frac{1}{k_p}(\dot{F} + k_d\ddot{x}) \\ &= \dot{x} + \frac{1}{k_p}\left[\dot{F} + \frac{k_d}{m}(F + F_{\text{ext}})\right] \\ \Rightarrow \dot{e}_d &= \dot{e} + \frac{1}{k_p}\left[\dot{F} + \frac{k_d}{m}(F + F_{\text{ext}})\right] \end{aligned} \quad (11)$$

Substituting the expression for the control force for Impedance Control from (3) in the above equation it is possible to obtain an expression of the form

$$X_a = S_{ai} X_i, \qquad S_{ai} = \begin{bmatrix} I \\ S \end{bmatrix} \quad (12)$$

where I is the identity matrix and entries of $S = [s_{ij}]_{2\times2}$ have the expressions

$$\begin{aligned} s_{11} &= 1 - \frac{k_e}{k_p}\left(\frac{m}{M_d} - 1\right) - \frac{K_d}{k_p}\frac{m}{M_d} \\ s_{12} &= \frac{k_d}{k_p} - \frac{D_d}{k_p}\frac{m}{M_d} \\ s_{21} &= -\frac{m}{M_d}\frac{(K_d + k_e)}{k_p}\left(\frac{k_d}{m} - \frac{D_d}{M_d}\right) \\ s_{22} &= 1 - \frac{k_e}{k_p}\left(\frac{m}{M_d} - 1\right) - \frac{D_d}{M_d}\left(\frac{k_d}{k_p} - \frac{D_d}{k_p}\frac{m}{M_d}\right) - \frac{K_d}{k_p}\frac{m}{M_d} \end{aligned} \quad (13)$$

When the system switches from Admittance to Impedance Control, the state variable mapping is given by the relation

$$X_i = S_{ia} X_a, \qquad S_{ia} = \begin{bmatrix} I & O \end{bmatrix} \quad (14)$$

where O is the 2×2 matrix with zero entries.

C. Stability Analysis

Knowing the states of the system at $t = t_0 + k\delta$, the states at time $t = t_0 + (k+1)\delta$, $k = 0, 1, 2, \cdots$ can be obtained using (10), (12) and (14) as follows

$$\begin{aligned} X_i(t_0 + (k+1-n)\delta) &= e^{A_i(1-n)\delta}X_i(t_0 + k\delta) \\ X_a(t_0 + (k+1-n)\delta) &= S_{ai} X_i(t_0 + (k+1-n)\delta) \\ X_a(t_0 + (k+1)\delta) &= e^{A_a n\delta}X_a(t_0 + (k+1-n)\delta) \\ X_i(t_0 + (k+1)\delta) &= S_{ia} X_a(t_0 + (k+1)\delta) \end{aligned} \quad (15)$$

$$\Rightarrow X_i(t_0 + (k+1)\delta) = \\ S_{ia} e^{A_a n\delta} S_{ai} e^{A_i(1-n)\delta} X_i(t_0 + k\delta) \quad (16)$$

We now define *Discrete Equivalent Subsystem* based on the definition of *Discrete Equivalent* in Das and Mukherjee [11].

Definition 1: Discrete Equivalent Subsystem (DES): The time-invariant linear system

$$\dot{X} = A_{\text{eq}}X \quad (17)$$

is a DES of a switched linear system if state variables of the DES assume identical values of a subset of the states of the switched system at regular intervals of time, starting from the same initial condition. ◇◇◇

Based on the above definition, the system described by (17) is a DES of the switched system described by (10), (12) and (14) with

$$A_{\mathrm{eq}} = \frac{1}{\delta} \ln[S_{ia} \, e^{A_a n \delta} S_{ai} \, e^{A_i (1-n)\delta}] \qquad (18)$$

Theorem 1: Exponential Stability[6]: The equilibrium $X_i = 0$ of the switched system described by Eqs.(10), (12) and (14) is exponentially stable if A_{eq} of the DE system in (18) is Hurwitz.

Proof: For convenience, we define the following norms:

$$\begin{aligned} \eta_1 &= \| A_i \| & c_1 &= \| S_{ai} \| \\ \eta_2 &= \| A_a \| & c_2 &= \| S_{ia} \| \end{aligned}$$

For the DE system, we assume $\| X(t_0) \| = \epsilon$. Since, A_{eq} is Hurwitz, we have

$$\begin{aligned} X(t) &= e^{A_{eq}(t-t_0)} X(t_0) \\ \implies \| X(t) \| &\leq \| e^{A_{eq}(t-t_0)} \| \, \| X(t_0) \| \\ &\leq \gamma e^{-\lambda(t-t_0)} \epsilon \end{aligned} \qquad (19)$$

where $\gamma, \lambda > 0$ are positive numbers. Assuming that the states of the switched system and its DE assume identical values at $t = t_0 + k\delta$, $k = 0, 1, 2, \cdots$, the states of the switched system satisfy

$$\| X_i(t_0 + k\delta) \| \leq \gamma \epsilon \, e^{-\lambda k \delta} \qquad (20)$$

Now consider the time interval $t_0 + k\delta \leq t \leq t_0 + (k+1)\delta$. Within this interval, first consider the subinterval $(t_0 + k\delta) \leq t \leq t_0 + k\delta + (1-n)\delta$ where Impedance Control is used. Using (20) and the relations $t = t_0 + k\delta + \tau_1$, $0 \leq \tau_1 \leq (1-n)\delta$, we have

$$\begin{aligned} X_i(t_0 + k\delta + \tau_1) &= e^{A_i \tau_1} X_i(t_0 + k\delta) \\ \Rightarrow \| X_i(t_0 + k\delta + \tau_1) \| &\leq \| e^{A_i \tau_1} \| \, \| X_i(t_0 + k\delta) \| \\ &\leq e^{\eta_1 \tau_1} \gamma \epsilon \, e^{-\lambda k \delta} \\ &\leq \gamma \epsilon \, e^{(\eta_1 + \lambda)\tau_1} \, e^{-\lambda(k\delta + \tau_1)} \\ \Rightarrow \| X_i(t) \| &\leq \gamma \epsilon \, e^{(\eta_1 + \lambda)(1-n)\delta} \, e^{-\lambda(t-t_0)} \end{aligned} \qquad (21)$$

From (21) we directly get

$$\| X_i(t_0 + k\delta + (1-n)\delta) \| \leq \gamma \epsilon \, e^{\eta_1 (1-n)\delta} \, e^{-\lambda k \delta} \qquad (22)$$

At $t = t_0 + k\delta + (1-n)\delta$, Admittance Control is invoked and X_a defines the new states of the system. Using (22) and the second relation in (15) we get

$$\begin{aligned} \| X_a(t_0 + k\delta + (1-n)\delta) \| &\leq \| S_{ai} \| \gamma \epsilon \, e^{\eta_1 (1-n)\delta} \, e^{-\lambda k \delta} \\ &= c_1 \gamma \epsilon \, e^{\eta_1 (1-n)\delta} \, e^{-\lambda k \delta} \end{aligned} \qquad (23)$$

Now consider the subinterval of time $(t_0 + k\delta + (1-n)\delta) \leq t \leq (t_0 + (k+1)\delta)$ where Admittance Control is used. For $t = t_0 + k\delta + (1-n)\delta + \tau_2$, $0 \leq \tau_2 \leq n\delta$, we have

$$\begin{aligned} X_a(t_0 + k\delta + (1-n)\delta + \tau_2) \\ = e^{A_a \tau_2} X_a(t_0 + k\delta + (1-n)\delta) \end{aligned}$$

Using (23) we get

$$\begin{aligned} \| X_a(t_0 + k\delta + (1-n)\delta + \tau_2) \| \\ \leq \| e^{A_a \tau_2} \| \, \| X_a(t_0 + k\delta + (1-n)\delta) \| \\ \leq e^{\eta_2 \tau_2} c_1 \gamma \epsilon \, e^{\eta_1 (1-n)\delta} \, e^{-\lambda k \delta} \end{aligned}$$

Using (14) we can write

$$\begin{aligned} \| X_i(t_0 + k\delta + (1-n)\delta + \tau_2) \| \\ \leq \| S_{ia} \| \, \| X_a(t_0 + k\delta + (1-n)\delta + \tau_2) \| \\ \leq c_2 \, e^{\eta_2 \tau_2} c_1 \gamma \epsilon \, e^{\eta_1 (1-n)\delta} \, e^{-\lambda k \delta} \\ \leq c_1 c_2 \gamma \epsilon \, e^{(\eta_1 + \lambda)(1-n)\delta} \, e^{(\eta_2 + \lambda)n\delta} \, e^{-\lambda(t-t_0)} \end{aligned} \qquad (24)$$

From (21) and (24) we deduce

$$\begin{aligned} \| X_i(t) \| &\leq \kappa e^{-\lambda(t-t_0)}, \\ \kappa &\equiv c_1 c_2 \gamma \epsilon \, e^{(\eta_1 + \lambda)(1-n)\delta} \, e^{(\eta_2 + \lambda)n\delta} \end{aligned} \qquad (25)$$

for $t \in [t_0 + k\delta, t_0 + (k+1)\delta]$, $k = 0, 1, 2, \cdots$, which implies exponential stability of $X_i = 0$. $\diamond\diamond\diamond$

IV. A CASE STUDY

A. Example System

We consider a single degree-of-freedom system in which the environment is modeled as a linear spring of stiffness k_{e}. The equation of motion of the mass m is given by

$$m\ddot{x} = F + F_{\mathrm{ext}} + F_f \qquad (26)$$

where $F_{\mathrm{ext}} = -k_{\mathrm{e}} x$ is the external force applied by the environment on the mass and F_f is the unmodeled friction which is assumed to have the form

$$F_f = -\mathrm{sign}(\dot{x})(c_v|\dot{x}| + F_c) \qquad (27)$$

with c_v and F_c as the coefficients of viscous and Coulomb friction. Impedance Control was implemented using (3) and (26) and Admittance Control was implemented using (4), (6) and (26). The parameter values used in our analysis are as follows:

$$m = 1.0 \, \mathrm{kg}, \quad \hat{m} = 0.8 \, \mathrm{kg}$$

$$c_v = 1.0 \, \mathrm{Ns/m}, \quad F_c = 3.0 \, \mathrm{N}$$

$$k_p = 10^6 \, \mathrm{N/m}, \quad k_d = 2 \times 0.7\sqrt{k_p m} \, \mathrm{Ns/m}$$

$$M_d = \hat{m}, \quad K_d = 100 \, \mathrm{N/m}, \quad D_d = 2 \times 0.7\sqrt{K_d M_d} \, \mathrm{Ns/m}$$

Modeling uncertainty is introduced in both implementations by considering the estimated mass $\hat{m}$ instead of the mass m. The (PD) position controller is designed with high gains, which is common practice, but modeling uncertainty of m is not considered since we can realistically assume that the position control loop is tuned independently. The simulations were based on a sampling time of 1 ms. It was assumed that feedback of external forces is affected by white noise[7] and an unmodeled time-delay of $T_d = 2$ ms.

---

[6]A slightly different version of this theorem and proof appears in the paper by Das and Mukherjee [11].

[7]The noise on the force signal is implemented using the "Band-Limited White Noise" block in Matlab/Simulink using a "noise power" value of 0.001.

B. Nominal Stability

In this section we assume the ideal model (1) without friction, noise, or modeling uncertainty. We assume a constant switching rate n and switching time δ. Figure 5 shows the result of a numerical stability analysis of the DES defined by (18) in dependence of n, δ, and k_e. The solid lines show the border lines between a stable and unstable closed loop system for different values of δ. The area at the lower left hand side of the lines represents the stable area. One can see that a smaller δ leads to a larger stable region. One might expect that all lines would end up at the stability border of the plain Admittance Controller for $n = 1$. However, this is not the case since the point $n = 1$ represents an admittance controller, which is being reset by condition (12) every time δ, rather than a pure Admittance Controller. For a large δ, the stability border of the controller with $n = 1$ tends to the stability border of the Admittance Controller. From this one can see that the periodic resetting of the Admittance Controller already improves its stability. Intuitively, this can be understood by considering the case of $\delta \to 0$, for which the resetting of the Admittance Controller results in Impedance Control. Moreover, one can see that for a smaller $n < 1$, the switching from Admittance Control to Impedance Control improves the stability even more.
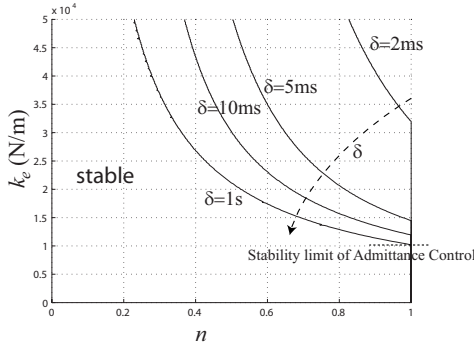
Fig. 5. Stability borders of the hybrid impedance admittance controller for different values of δ.

Figure 5 confirms the main design idea of using a periodic switching between Impedance and Admittance Control from a stability point of view. However, by analyzing the influence of δ more carefully, a surprising effect can be observed. Figure 6 shows the same stability borders as in Fig. 5, but for $\delta = 15\ ms$ and $\delta = 20\ ms$. In addition to the expected stability improvement for smaller values of n, we can observe an increased unstable region around a certain value of k_e. Consider for instance the case $n = 0.4$, $\delta = 20\ ms$. If we increase the external stiffness from $2 \cdot 10^4 N/m$ to $2.5 \cdot 10^4 N/m$ the system becomes unstable. But if we increase the stiffness further to $3 \cdot 10^4 N/m$ the system becomes stable again. While this is not intuitive, it should be mentioned that this effect can indeed be verified by simulations. The origin and meaning of this interesting effect is currently topic of further investigation.
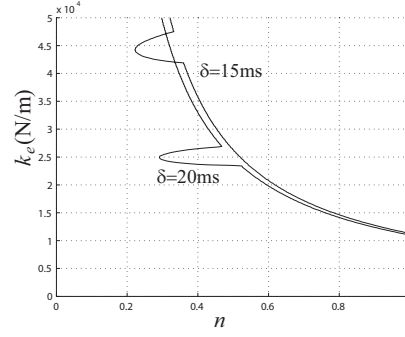

Fig. 6. Stability borders of the hybrid impedance admittance controller for different values of δ.

C. Performance

We highlight the performance and stability properties of the hybrid controller by simulating a step change in the virtual equilibrium position x_0 from zero to 1 m (while setting $\ddot{x}_0 = \dot{x}_0 = 0$) for a soft, an intermediate, and a stiff environment. To simulate the soft, intermediate and stiff environments, k_e was chosen as 10 N/m, 300 N/m and 3200 N/m, respectively.

The ideal behavior of the closed-loop system, denoted by x_{ref}, is obtained from (2)

$$M_d\,\ddot{x}_{\text{ref}} + D_d\,\dot{x}_{\text{ref}} + (K_d + k_e)x_{\text{ref}} = K_d\,x_0 \qquad (28)$$

and is plotted in Fig.7. Since different values of k_e result in different final values of x_{ref}, we plot the normalized value of x_{ref} in Fig. 7. Notice that in this comparison we keep the damping of the desired impedance constant, and do not adapt it to the environment stiffness. This results in different damping characteristics, i.e. low damping for stiff contact and higher damping for soft contact. Figure 8 shows the deviation of x from its ideal trajectory for the different controllers with the soft environment ($k_e = 10$ N/m). It can be seen that Admittance Control results in good performance whereas Impedance Control results in tracking errors and a steady state error due to uncompensated friction. For the hybrid controller, a switching period of $\delta = 20ms$ was chosen and Fig. 8 shows the results for different values of the switching rate n. One can see that the switching rate can be used to generate different closed loop behaviors between Impedance and Admittance Control. In addition, in Fig. 9 the result for different values of the switching period with $n = 0.5$ is shown.

The results for the environment with intermediate stiffness ($k_e = 300$ N/m) are shown in Fig.10. By comparing these results with those in Fig.8 it is clear that Impedance Control results in improved performance with reduced steady state error but the performance of the system deteriorates with Admittance Control. It deteriorates further for the stiff environment ($k_e = 3200$ N/m), which is evident from the large oscillations in Fig.11. This can be attributed to the high gains of the underlying position (PD) controller and the time-delay of force feedback. For the stiff environment, Impedance Control however provides very good performance with negligible steady state error.
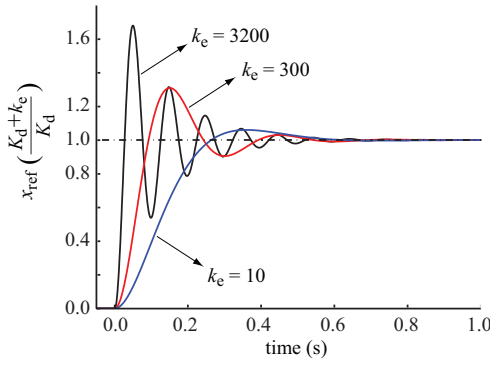
558

Fig. 7. Ideal trajectories of the mass for a step change in the virtual equilibrium position for a soft, an intermediate and a stiff environment
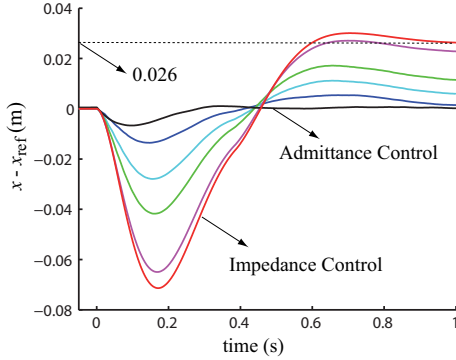

Fig. 8. Deviation in trajectory of mass from its ideal trajectory for the soft environment $k_e = 10$ N/m. The lines in magenta, green, cyan, and blue color show the result of the hybrid controller with $n = 0.2$, $n = 0.4$, $n = 0.6$, and $n = 0.8$, respectively.
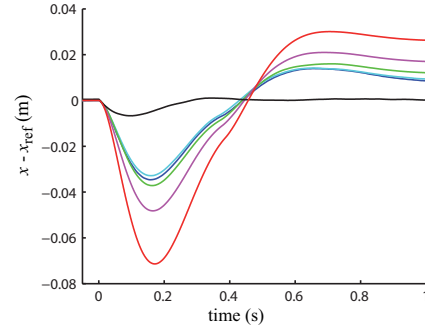

Fig. 9. Deviation in trajectory of mass from its ideal trajectory for the soft environment $k_e = 10$ N/m. The lines in magenta, green, cyan, and blue color show the result of the hybrid controller with $\delta = 2ms$, $\delta = 4ms$, $\delta = 10ms$, and $\delta = 20ms$, respectively.
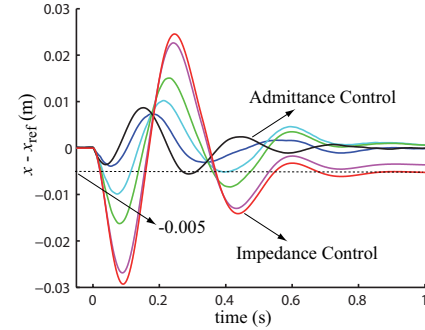

Fig. 10. Deviation in trajectory of mass from its ideal trajectory for environment stiffness $k_e = 300$ N/m. The lines in magenta, green, cyan, and blue color show the result of the hybrid controller with $n = 0.2$, $n = 0.4$, $n = 0.6$, and $n = 0.8$, respectively.

By comparing Fig. 8 and Fig. 11, one can see that by proper choice of n, the hybrid controller leads to smaller steady state error than Impedance Control and a more robust behavior in stiff contact than Admittance Control.

In the simulations so far we considered constant values of n and δ. Clearly, if the stiffness of the environment is known (or can be observed), the switching rate can also be adapted to the contact stiffness in order to achieve a stable motion in stiff contact and good position accuracy in soft contact (or even free motion). This is shown in the next simulation. First, a step response is performed for a stiff contact ($k_e = 2500 \ N/m$). At time 1.5s the contact stiffness is continuously changed according to Fig. 12. The corresponding desired motion x_{ref} is shown in Fig. 13.

Figure 14 shows the results of the hybrid controller with $\delta = 20 \ ms$ and $n = 0.5$ compared to the behavior of the Impedance and Admittance Controller. Here one can clearly observe that at the first part of the motion, i.e. during stiff contact, the behavior of the Impedance Controller is better, while for the second part, i.e. during soft contact, the behavior of the Admittance Controller is better. Notice that the error of the admittance controller in the second part is due to the simulated noise on the force signal. As expected, the hybrid controller with $n = 0.5$ gives a result in between Impedance and Admittance Control. It allows to improve (compared to Impedance Control) the steady state accuracy during soft contact and perform stable motion during stiff

contact.

Finally, if we assume that the environment stiffness is known (or can be observed), we can adapt the switching rate n to the stiffness. Therefore, we can effectively combine the strength of Impedance and Admittance in one hybrid controller. Figure 15 shows the error of the hybrid controller for an adjustment of n via the simple adaption law $n = 1 - k_e(t)/2500$. Here we can see that online adaption of n allows to optimize the behavior of the hybrid controller in a continuous way.

V. EXPERIMENTAL EVALUATION

In this section we present a first experimental evaluation of the presented hybrid control framework. As an experimental platform, we used the KUKA-DLR-Lightweight arm (Fig. 16) equipped with a JR3 force/torque sensor at the tip. In particular, we utilize the torque control interface of this arm and implement both Impedance and Admittance Control with a sampling rate of 1ms around the robot's inner loop torque control. For the implementation of Admittance Control we did not use the 'built-in' position controller running at a faster control loop, so that both Impedance and Admittance Control are executed at the same sampling level as considered in the analysis of this paper. The utilization of faster inner control loops in the hybrid framework is topic of further research.
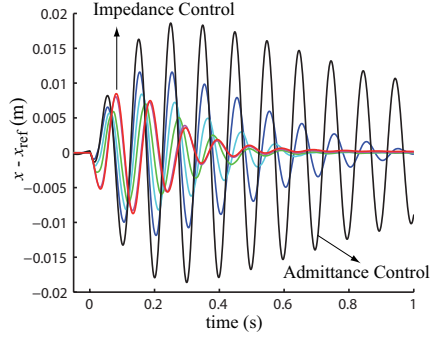
Fig. 11. Deviation in trajectory of mass from its ideal trajectory for the stiff environment $k_e = 3200$ N/m. The lines in magenta, green, cyan, and blue color show the result of the hybrid controller with $n = 0.2$, $n = 0.4$, $n = 0.6$, and $n = 0.8$, respectively.
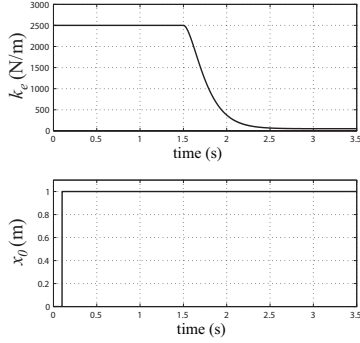

Fig. 12. Time varying stiffness k_e and commanded equilibrium position x_0.

We implemented the hybrid controller for the elbow joint of the robot. The control parameters are given by

$$\hat{m} = 0.433 \,\frac{\text{Nms}^2}{\text{rad}}, \;\; k_p = 5000 \,\frac{\text{Nm}}{\text{rad}}, \;\; k_d = 15 \,\frac{\text{Nms}}{\text{rad}}$$

$$M_d = \hat{m} \;\; K_d = 100 \,\text{N/m}, \;\; D_d = 2 \times 0.7 \sqrt{K_d M_d} \,\text{Ns/m}$$

We present a contact experiment in which we command the elbow joint such that the end-effector gets in contact with the robot's supporting table (see Fig. 16). The commanded virtual equilibrium position is shown in Fig. 17 together with the trajectories resulting from Impedance (red) and Admittance (blue) Control. Figure 18 and 19 show the errors $x - x_0$ for the two controllers. One can see that the Admittance controller shows an oscillation during stiff contact, but has good position accuracy in free steady state. Impedance Control instead shows a larger steady state error in free motion. Figure 20 finally shows the result of the hybrid controller with $\delta = 20ms$ for different values of the switching rate n. One can see that no oscillation occurs for the hybrid controller in stiff contact. The controller with $n = 0.9$ shows about half of the steady state error as compared to Impedance Control. This evaluation of the hybrid controller on a single joint confirms that it is possible to reduce the steady state error of Impedance Control and to improve the stability of Admittance Control by the proposed hybrid control approach.
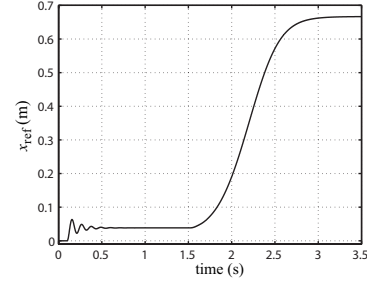

Fig. 13. System motion x_{ref} according to the desired impedance behavior for the varying contact stiffness.
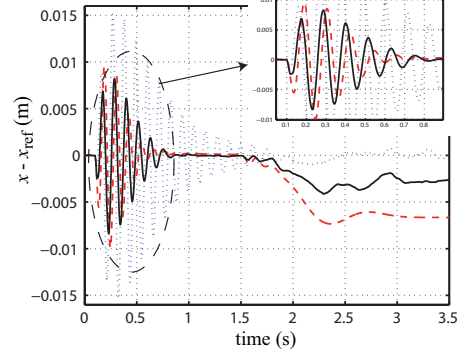

Fig. 14. Comparison of the hybrid controller with constant $n = 0.5$ (black solid line) to the errors of Impedance (red dashed line) and Admittance Control (blue dotted line).

VI. Summary and Outlook

In this paper, we presented a new solution to the impedance control problem in which we constantly switch between controllers with admittance and impedance causality. By taking the switching time and period as design parameters, we get a family of controller, which includes classical Impedance and Admittance Control as extreme cases and, moreover, allows to continuously interpolate between them. This approach allows to effectively combine the accuracy of Admittance Control in free motion with the robustness properties of Impedance Control in stiff contact in one single control framework.

The analysis in this paper was focused on a single degree-of-freedom case study. However, we think that the extension to the nonlinear multi degree-of-freedom case is possible and it is a domain of our further investigations.
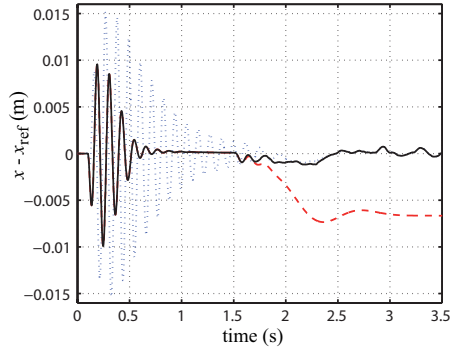
Acknowledgment

Fig. 15. Comparison of the hybrid controller with online adjusted n (black solid line) to the errors of Impedance (red dashed line) and Admittance Control (blue dotted line).
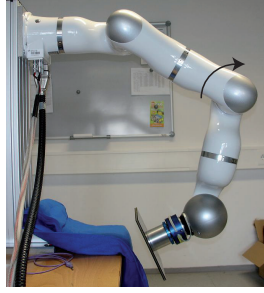

Fig. 16. Experimental setup.

REFERENCES

[1] M. Raibert and J. Craig, "Hybrid position/force control of manipulators," *ASME Journal of Dynamical Systems, Measurement and Control*, vol. 105, pp. 126–133, 1981.

[2] M. Mason, "Compliance and force control for computer controlled manipulators," *IEEE Transactions on Systems, Man, and Cybernetics*, vol. 11, no. 6, pp. 418–432, 1981.

[3] N. Hogan, "Impedance control: An approach to manipulation, part I - theory," *ASME Journal of Dynamic Systems, Measurement, and Control*, vol. 107, pp. 1–7, 1985.

[4] R. Anderson and M.W.Spong, "Hybrid impedance control of robotic manipulators," *IEEE Transactions on Robotics and Automation*, vol. 4, no. 5, pp. 549–556, 1988.

[5] G. Liu and A. Goldenberg, "Robust hybrid impedance control of robot manipulators," in *IEEE International Conference on Robotics and Automation*, 1991, pp. 287–292.

[6] D. Lawrence, "Impedance control stability properties in common implementations," in *IEEE International Conference on Robotics and Automation*, 1988, pp. 1185–1190.

[7] Ch. Ott, O. Eiberger, W. Friedl, B. Bäuml, U. Hillenbrand, Ch. Borst, A. Albu-Schäffer, B. Brunner, H. Hirschmüller, S. Kielhöfer, R. Konietschke, M. Suppa, T. Wimböck, F. Zacharias, and G. Hirzinger, "A humanoid two-arm system for dexterous manipulation," in *IEEE-RAS International Conference on Humanoid Robots*, 2006, pp. 276–283.

[8] G. Cheng, S.-H. Hyon, J. Morimoto, A. Ude, G. Colvin, W. Scroggin, and S. C. Jacobsen, "Cb: A humanoid research platform for exploring neuroscience," in *HUMANOIDS*, 2006.

[9] D. Liberzon and A. S. Morse, "Basic problems in stability of switched systems," *IEEE Control Systems Magazine*, pp. 59–70, 1999.

[10] T. Valency and M. Zacksenhouse, "Accuracy/robustness dilemma in impedance control," *ASME Journal of Dynamic Systems, Measurement, and Control*, vol. 125, pp. 310–319, 2003.

[11] T. Das and R. Mukherjee, "Shared-sensing and control using reversible transducers," *IEEE Transactions on Control Systems Technology*, vol. 17, pp. 242–248, 2009.
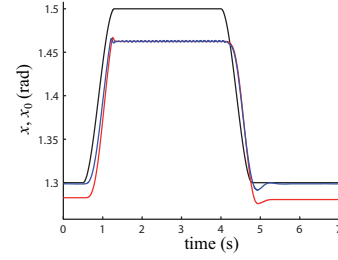
Fig. 17. Virtual Equilibrium position (black) and resulting trajectories with Impedance (red) and Admittance (blue) control.
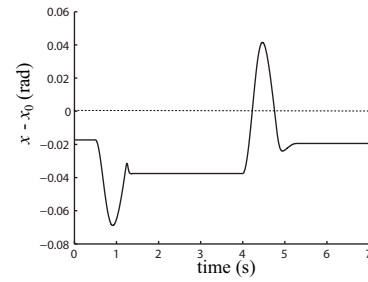

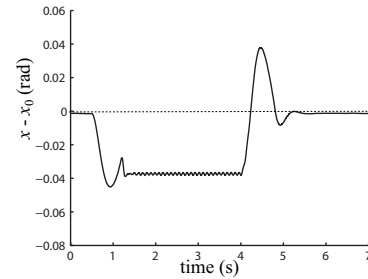Fig. 18. Experimental result with Impedance Control.

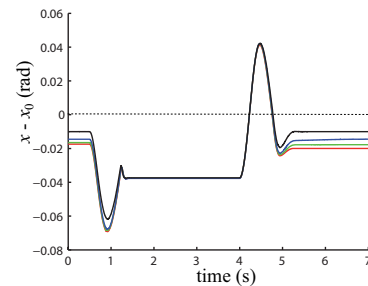Fig. 19. Experimental result with Admittance Control.

Fig. 20. Experimental result with the hybrid controller. The red, green, blue, and black lines show the results for $n = 0.2$, $n = 0.5$, $n = 0.65$, $n = 0.9$, respectively.

561